Available online at www.sciencedirect.com
ScienceDirect
Journal of Magnetic Resonance 183 (2006) 315–323
JMR Journal of Magnetic Resonance
www.elsevier.com/locate/jmr

Communication

Observation of anomalous diffusion in excised tissue by characterizing the diffusion-time dependence of the MR signal

Evren Özarslan [a,*], Peter J. Basser [a], Timothy M. Shepherd [b], Peter E. Thelwall [b,c], Baba C. Vemuri [d], Stephen J. Blackband [b,e]

[a] STBB/LIMB/NICHD, National Institutes of Health, Bethesda, MD 20892, USA
[b] Department of Neuroscience, University of Florida, Gainesville, FL 32610, USA
[c] Newcastle Magnetic Resonance Center, University of Newcastle, Newcastle upon Tyne, UK
[d] Department of Computer and Information Science and Engineering, University of Florida, Gainesville, FL 32611, USA
[e] National High Magnetic Field Laboratory, Tallahassee, FL 32310, USA

Received 9 May 2006; revised 7 August 2006
Available online 8 September 2006

Abstract

This report introduces a novel method to characterize the diffusion-time dependence of the diffusion-weighted magnetic resonance (MR) signal in biological tissues. The approach utilizes the theory of diffusion in disordered media where two parameters, the random walk dimension and the spectral dimension, describe the evolution of the average propagators obtained from q-space MR experiments. These parameters were estimated, using several schemes, on diffusion MR spectroscopy data obtained from human red blood cell ghosts and nervous tissue autopsy samples. The experiments demonstrated that water diffusion in human tissue is anomalous, where the mean-square displacements vary slower than linearly with diffusion time. These observations are consistent with a fractal microstructure for human tissues. Differences observed between healthy human nervous tissue and glioblastoma samples suggest that the proposed methodology may provide a novel, clinically useful form of diffusion MR contrast.

Keywords: Diffusion time; Power-law; Disordered media; Fractal; Scaling; Walk dimension; Spectral dimension; Fracton

1. Introduction

Magnetic resonance (MR) imaging or spectroscopy measurements of the translational self-diffusion of water molecules have found widespread use in biophysical investigations of materials and biological tissues [1]. Water diffusion behavior in tissue can be observed via magnetic resonance from multiple experimental perspectives and modeled in different mathematical fashions. Clinically, simple diffusion-weighted MRI has proven to be highly sensitive to tissue microstructure changes that correlate with acute tissue injury, particularly in ischemic brain injury or stroke [2]—this has proven utility for making treatment decisions in the treatment of stroke patients [3]. MR measurement of the orientational dependence of water diffusion in nervous tissue also has proven useful for the detection of coherent, anisotropically oriented white matter structures in the human brain [4]. In most published studies that involve diffusion MR, one observes the MR signal intensity dependence based on the magnitude or orientation of applied diffusion sensitizing gradients. However, some studies have suggested additional information about tissue microstructure can be obtained if other parameters of the experiment, such as the diffusion time, were also varied [5,6]. This paper will demonstrate novel, previously unrecognized information that is obtainable from q-space diffusion MR studies of biological tissues.

* Corresponding author. Fax: +1 301 435 5035.
E-mail address: evren@helix.nih.gov (E. Özarslan).

1090-7807/$ - see front matter © 2006 Elsevier Inc. All rights reserved.
doi:10.1016/j.jmr.2006.08.009

Extracting structural information from the diffusion-attenuated MR signal requires models of biological tissue [7] that link biophysical features of the underlying microstructure to the measured diffusion-weighted MR signal. Previous models of the biophysical relationship between tissue microstructure and water diffusion observed experimentally have assumed (or by computational necessity required) that the tissue under investigation be described simply with cells that are simple cylinders or spheres and that the simple geometric constructs create multiple unique water compartments [8–10]. Another example is the application of the diffusion tensor model originally developed for liquid crystals to describe the signal attenuation in nervous tissue environments with structural anisotropy [4]. Valuable and clinically useful information has been obtained from these models. However, it is well-known that neurons and glia are not uniformly sized spheres or cylinders and that subsequent combined populations of neurons and glia in a holistic tissue environment have a more complicated architecture on several different length scales than the above models were able to envision. Previous studies have demonstrated that neurons have a fractal-like appearance [11,12], and the fractal dimension, as a measure of complexity, can be indicative of the different cell types [13,14]. In this paper, we report a novel mathematical model of water diffusion that accounts for some of the microstructural complexity probed by water diffusing in nervous tissue on several different length scales—the barriers to water diffusion presented by cellular organelles and cytoskeletal proteins, by the complex shapes of nervous tissue cells, and by the complex spatial arrangements of neurons and glia in tissue.

Anomalous diffusion is a well-known phenomenon in statistical physics in which the mean squared displacement of the diffusing particles has a nonlinear scaling behavior with time. This process occurs in systems exhibiting fractal behavior [15], such as percolation clusters [16,15,17,18], where there are restrictions to diffusion at different length scales. There have been several NMR studies in which the anomalous behavior of water diffusion in nonbiological materials have been quantified accurately [19–21]. q-space MR experiments provide a noninvasive means to compute an ensemble average propagator associated with the diffusion process [7,22–24]. Because the length scales that can be probed using pulsed field gradient (PFG) experiments coincide with those that restrict the molecular motion of water in tissue, it may be possible to create a novel MR contrast mechanism based on the evolution of these average propagators as a function of diffusion time. In this paper our goal was to demonstrate the feasibility of estimating the scaling exponents that characterize anomalous diffusion in disordered media from q-space MR measurements. To investigate this point and understand how well such an approach characterizes the time evolution of average propagators, we show experimental findings from q-space spectroscopy data obtained from three unique human tissue samples.

2. Theory

The diffusion process in disordered media and systems exhibiting fractal behavior is anomalous. This is the case when the mean-square displacement (MSD) of the diffusing particles has a diffusion time (t) dependence characterized by the power-law

$$\mathrm{MSD} = \langle r^2 \rangle \propto t^{2/d_w} \tag{1}$$

with $d_w \neq 2$, where d_w is the walk (or path or trail) dimension quantifying the fractal dimension of the paths followed by the randomly moving particles. The MSD, $\langle r^2 \rangle$, is related to the square of the characteristic length associated with the diffusion process. When $d_w = 2$, the diffusion process is "normal" whereas in the case when $d_w > 2$, the distances traveled by the particles have a slower-than-linear time dependence. This kind of a process is called subdiffusion. The opposite case ($d_w < 2$) corresponds to a faster-than-normal diffusion process which is called superdiffusion. Various systems that give rise to these different behaviors are discussed in [15].

Another scaling exponent that characterizes the scaling behavior of the density of states function for the Laplacian operator is called the spectral (fracton) dimension and will be denoted by d_s. The return-to-origin probability (RTOP) [25] for diffusing particles obeys a power-law characterized by d_s via the expression [15]

$$\mathrm{RTOP} = P(r = 0, t) \propto t^{-d_s/2}, \tag{2}$$

where $P(r,t)$ is the probability for the particles to move a distance r in time t. For normal diffusion $d_s = d$, where d is the embedding dimension.[1] In fractals, the fractal dimension d_f, is related to the walk and spectral dimensions through the relationship

$$d_f = \frac{d_w d_s}{2}. \tag{3}$$

A reasonable form of the propagator $P(r,t)$ that incorporates these scaling relations is given by [15,26]

$$P(r,t) \propto \frac{r^{d_f - d}}{t^{d_s/2}} \Phi\left(\frac{r}{t^{1/d_w}}\right), \tag{4}$$

where the argument of the function Φ ensures the scaling relation given in Eq. (1). The numerator $r^{d_f - d}$ is related to the scaling of the "mass" of the fractal with distance and the denominator $t^{d_s/2}$ is necessary for the time independence of the total probability. One can immediately show that the radial moments of $P(r,t)$ have the scaling behavior

$$\langle r^m \rangle = 4\pi \int P(r,t) r^{2+m} \, \mathrm{d}r, \tag{5}$$

$$\propto t^{m/d_w}. \tag{6}$$

Consequently, $1/d_w$ characterizes all moments of the distribution and is called a "gap exponent". However, more generally,

[1] Note that d is an integer.

the moments of the distribution can be characterized by a hierarchy of exponents [26] in which case Eq. (4) is not valid.

In a one-dimensional PFG experiment, an ensemble averaged water displacement probability function $\overline{P}_1(z,\Delta)$ is related to the MR signal attenuation $E(q,\Delta)$ through the relationship

$$\overline{P}_1(z,\Delta) = \int_{-\infty}^{\infty} E(q,\Delta)\mathrm{e}^{-2\pi i q z}\,\mathrm{d}q, \tag{7}$$

where Δ is the separation time of the two diffusion gradients and $q = \gamma\delta G/2\pi$, where γ is the gyromagnetic ratio, δ is the diffusion pulse duration assumed to be much smaller than Δ, and G is the magnitude of the diffusion gradient whose direction defines the z-axis. Therefore, the water displacement probabilities can be computed from the signal attenuations via a discrete Fourier transform. Note that $\overline{P}_1(z,\Delta)$ is the projection of the three-dimensional average propagator, $\overline{P}(r,\Delta)$ onto the z-axis. In isotropic space, this projection is given simply by

$$\overline{P}_1(z,\Delta) = 2\pi\int_z^{\infty} \overline{P}(r,\Delta) r\,\mathrm{d}r. \tag{8}$$

It is straightforward to show that the radial moments of the isotropic three dimensional density $\overline{P}(r,\Delta)$ are proportional to the moments of $\overline{P}_1(z,\Delta)$. Therefore, the scaling behavior of the MSD values computed from both of these functions are characterized by the same exponent d_w. In order to estimate the MSD, one may use the relationship

$$\langle z^2\rangle = \int_{-\infty}^{\infty} \overline{P}_1(z,\Delta) z^2\,\mathrm{d}z \tag{9}$$

$$\frac{1}{2\pi^2}\lim_{q\to 0}\left(\frac{\partial \log E(q,\Delta)}{\partial q^2}\right) = 2D(\Delta)\Delta, \tag{10}$$

where $D(\Delta)$ is a diffusion-time dependent diffusion coefficient [27].

Note that a comparison of Eq. (8) with Eq. (5) implies that $\overline{P}_1(0,\Delta)$ is proportional to $\langle r^{-1}\rangle$. Therefore, it follows from Eq. (6) that if one assumes the three-dimensional probability density to be of the form in Eq. (4), then the $z = 0$ value of the projected propagator obeys the scaling behavior $\overline{P}_1(0,\Delta) \propto \Delta^{-1/d_w}$. In fact, inserting Eq. (4) into Eq. (8) would imply the following scaling relation for the projected probability density:

$$\overline{P}_1(z,\Delta) \propto \frac{1}{\Delta^{1/d_w}}\Psi\left(\frac{z}{\Delta^{1/d_w}}\right). \tag{11}$$

Therefore, the scaling behavior of the one-dimensional projection of the propagator is fully characterized by the walk dimension[2] if Eq. (4) holds for the three-dimensional propagator.

In this work, we will assume a slightly different form for the projected probability density where we "relax" the scaling condition on $\overline{P}_1(0,\Delta)$ and write

$$\overline{P}_1(z,\Delta) \propto \frac{z^{d'_f-1}}{\Delta^{d'_s/2}}\Psi\left(\frac{z}{\Delta^{1/d_w}}\right), \tag{12}$$

where d'_s is an effective spectral dimension, describing the scaling of the integral of the probabilities over an infinite plane that goes through the origin,[3] i.e.

$$\overline{P}_1(z=0,\Delta) = \int_{-\infty}^{\infty} E(q,\Delta)\,\mathrm{d}q, \tag{13}$$

$$\propto \Delta^{-d'_s/2}, \tag{14}$$

and d'_f is given by $d'_f = d_w d'_s/2$.

The estimation of the spectral dimension, d_s is also possible using PFG experiments and requires the estimation of the RTOP values. However, since the probability density at the origin is not readily available from the projected propagator, one has to consider the three-dimensional propagator, which is related to the signal attenuations via a three-dimensional Fourier transform. In isotropic space the RTOP values can be computed from the MR signal attenuation using the relationship

$$\mathrm{RTOP} = 4\pi\int_0^{\infty} E(q,\Delta) q^2\,\mathrm{d}q. \tag{15}$$

3. Methods

We have performed q-space spectroscopy experiments on three different samples. One of the samples was cerebral cortex from a normal person. The second sample was a human glioblastoma multiforme tumor (or grade-4 astrocytoma). Finally, the third sample was a human erythrocyte ghost model [28] prepared as described in [29]. The experiments were performed using a 14.1-T Bruker Avance spectrometer equipped with a gradient coil system that is capable of producing 3 T/m gradients along each of the three orthogonal directions. A diffusion-weighted stimulated echo pulse sequence was used that made it possible to span very long diffusion times. The spectroscopy data from the brain samples were acquired with TR/TE values of 4 s/11 ms. The echo was sampled with 2048 points. A total of 129 q-values were used for each diffusion time, where all three gradients were applied simultaneously yielding gradient strengths of up to 4892.5 mT/m. This sampling corresponded to a q-space resolution of 2 μm. The gradient duration (δ) was 2.4 ms, and we repeated the q-space measurements 12 times varying the gradient pulse separation

[2] The function $\Psi(\zeta)$ is related to the function $\Phi(\rho)$ via the integral

$$\Psi(\zeta) \propto \int_{\zeta}^{\infty} \Phi(\rho)\rho^{d_f-2}\,\mathrm{d}\rho.$$

Therefore, d_f—hence d_s—affects the form of the function $\Psi(\zeta)$, but not its scaling.

[3] When one assumes the three-dimensional propagator to obey the scaling behavior in Eq. (4), it is possible to see by comparing Eqs. (12) and (11) that $d'_w = d_w, d'_f = 1$, and $d'_s = 2/d_w$. Another interesting case occurs when the three-dimensional propagator is separable, i.e. when it is possible to write $P(r,t) = P_1(x,t)P_1(y,t)P_1(z,t)$. In this case, d_s is just three times d'_s. However, for more general forms of the propagators, these relations do not hold.

(Δ) between 12 and 613 ms on a logarithmic scale. A slightly different protocol was used to scan the erythrocyte ghost sample since the signal attenuated more rapidly with increasing gradient strengths. TR was set to 5 s, the maximum gradient strength used was 4194 mT/m and δ was 2 ms, giving rise to a q-space resolution of 2.8 μm. The q-axis was sampled on 65 points. All other parameters were identical to the acquisitions performed on the brain samples.

4. Results

We have employed several methods to estimate the scaling exponents d_w and d_s from excised tissue samples. Since, the MSD is proportional to the derivative of the logarithm of the signal at the origin of q-space (see Eq. (10)), the simplest method to estimate MSD is to compute a two point difference of $\log E(q,\Delta)$ near the origin. Then a double logarithmic plot of MSD vs. Δ is expected to be a straight line with slope $2/d_w$. However, it is important to do this in a consistent and acceptable manner for all time points, otherwise a bias from the nonlinearity of $\log E(q,\Delta)$ as a function of q^2 will be introduced. In this work, we present results obtained using several methods. In the first estimation, we chose one of the points to be the $q = 0$ data point, whereas the second data point was taken to be the one corresponding to a fixed q-value of 3.905 mm^{-1}. Fig. 1 shows the fits obtained using this constant-q method. We have also computed the MSD values by fixing the b-value of the second data point to 1000 s/mm^2. When data was not available at these locations, a cubic spline interpolation was used.

Note that d_w values can also be estimated from the average propagators computed from the Fourier transform given in Eq. (7) together with the integration in Eq. (9). The accuracy of the integral may be improved by using interpolated data in the displacement domain [30], which can be achieved by extrapolating the data points in q-space. Such an extrapolation scheme is obtained using a functional fit as described in the Appendix A.

A final estimation method aimed to minimize the effect of bias due to noise. This approach was based on the observation that the entire data set can be visualized on a Δ–q plane. For small values of q, one expects a quadratic dependence of $\log E(q,\Delta)$ on q. Therefore, the contours of the signal values on the Δ–q plane, near the Δ-axis are described by setting $q^2\langle z^2\rangle$ value to a constant. Since $\langle z^2 \rangle$ is expected to obey Eq. (1), an equivalent expression is $q^2\Delta^{2/d_w} = \text{constant}$. Taking the logarithm of both sides yields

$$\log q = C - \frac{1}{d_w}\log \Delta, \tag{16}$$

where C is a constant. Therefore, d_w can be estimated from the slope of the constant-E contours in the small-q region of the Δ–q plane. Fig. 2 depicts this method on the data set collected from the tumor sample. In this figure, the grayscale background shows the entire data set, where a histogram equalization was performed to increase the contrast. The curves depict the iso-attenuation contours computed using the "CONTOUR" routine of IDL (Research Systems Inc., Boulder, Colorado). As expected, these curves are linear near the Δ-axis on the Δ–q plane. The first few points in the low-q regime of 12 different contours were used in fitting a line, and the mean value of the 12 slopes was reported as the d_w value.

The d_w values estimated using these methods are presented in Table 1. Constant-q, constant-b, integration, and integration from extrapolated data methods all yielded fits with correlation coefficients above 0.999. The increased standard deviations indicate that the quality of the fits for the constant-E method was a bit poorer. However, for all three samples, the mean value obtained using this method was consistent with those obtained from the other approaches. The scaling laws in the healthy and tumor human tissue samples clearly indicated subdiffusive behavior, and the scaling of the characteristic length was faster in the tumor tissue. For the erythrocyte ghost sample, d_w values obtained using different schemes varied around the value

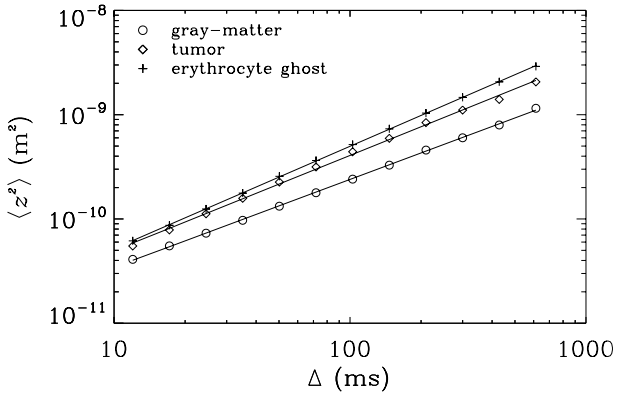

Fig. 1. Dependence of the mean squared displacements on diffusion time. The $\langle z^2\rangle$ values in this plot were computed using the constant-q method.

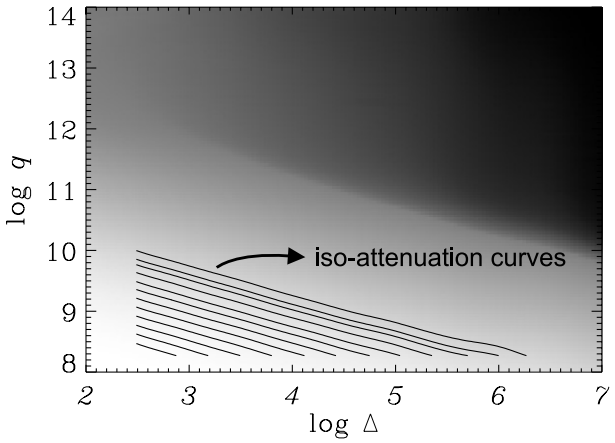

Fig. 2. Iso-attenuation curves on a $\log q$ vs. $\log \Delta$ plane overlaid on an "image" of the entire data set from the tumor sample. The curves depict the constant values of the MR signal and are used in the estimation of d_w (see Eq. (16)).

Table 1
d_w, d_s, and d'_s values estimated from three samples using various methods

	Estimation method	Gray-matter	Tumor	Erythrocyte ghost
d_w	Constant-q	2.371 ± 0.014	2.189 ± 0.029	2.036 ± 0.005
d_w	Constant-b	2.353 ± 0.013	2.188 ± 0.031	1.939 ± 0.017
d_w	Constant-E	2.376 ± 0.285	2.217 ± 0.369	2.021 ± 0.061
d_w	Integration	2.374 ± 0.014	2.183 ± 0.031	1.948 ± 0.033
d_w	Integration with extrapolation	2.394 ± 0.015	2.195 ± 0.028	2.038 ± 0.005
d_w	Fitting Eq. (17)	2.353 ± 0.041	2.183 ± 0.030	2.008 ± 0.013
d_s	Integration	$3.166 \pm .210$	$1.909 \pm .091$	$4.852 \pm .233$
d_s	Integration with extrapolation	$3.408 \pm .283$	$2.140 \pm .144$	$4.879 \pm .269$
d'_s	Integration	$0.991 \pm .008$	$1.018 \pm .009$	$1.312 \pm .036$
d'_s	Integration with extrapolation	$1.018 \pm .010$	$1.105 \pm .012$	$1.353 \pm .039$

of 2.0. Most likely, diffusion process in this sample was nonfractal. This is an expected result as the water molecules encounter only the cellular membranes that restrict the water molecular motion at only one length scale.

Another alternative to the d_w estimation is to fit a curve to the signal values directly. This method may be preferable since it may allow one to incorporate the effects of the finite pulse width. There are a number of attempts in the literature to relate the MR echo intensity to the scaling exponent d_w [31–35]. Among these, in Ref. [34], the following relationship for PFG experiments was provided that takes the finite pulse width into account[4]:

$$E(q,\Delta) = \exp\left\{-\frac{4\pi^2\gamma^2G^2\alpha}{3(\kappa+1)(\kappa+2)} \times\left[\frac{1}{2}(\Delta+\delta)^{\kappa+2}+\frac{1}{2}(\Delta-\delta)^{\kappa+2}-\Delta^{\kappa+2}-\delta^{\kappa+2}\right]\right\}, \quad (17)$$

where α is a generalized diffusion coefficient and $\kappa = 2/d_w$. We have applied a Levenberg–Marquardt fitting procedure to the data values at $q = 3.905\ \text{mm}^{-1}$. The fitting was very sensitive to the initial values of the parameters to be estimated. However, when the initial values are chosen to be close to the values obtained from other techniques, the estimates of d_w from the fits were consistent with the other estimates (see Table 1). Fig. 3 shows these fits.

The d_s values were estimated from the slope of the lines fitted to the RTOP values plotted as a function of Δ on a double logarithmic plot. The computation of the RTOP values involved the evaluation of the integral in Eq. (15) using a five-point Newton–Cotes formula. In order to reduce the effect of the finite window size in q-space, the fitting was repeated for the RTOP values obtained from the extrapolated data (see Appendix A). The same scheme was applied to estimate the d'_s values where the integral in Eq. (13) was computed using the same Newton–Cotes procedure. Fig. 4 shows the fits obtained for both d_s and d'_s estimations when extrapolation was not performed. Higher quality fits were obtained in the estimation of d'_s with correlation coefficients greater than 0.99. Although

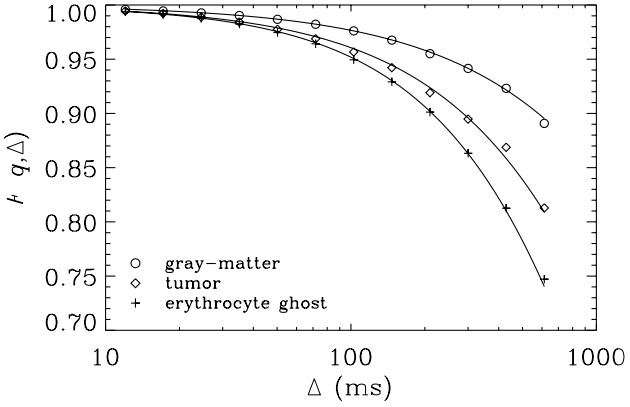

Fig. 3. Signal attenuation values with increasing diffusion times. The solid lines indicate the curves obtained by fitting Eq. (17).

the correlation coefficients were still larger than 0.97 for the RTOP fits, a visual examination of the points and the fitted lines suggests that the deviations from the expected power-law behavior might be due to systematic factors—most notably in the erythrocyte ghost sample. It is typical for real life systems to exhibit a power-law behavior only for a limited range of length or time scales [12] or obey different power-laws at different scales [36]. This may contribute to a reduction in the quality of fits as well as the deviation of the estimated d_s value from its "normal" value of 3 in the erythrocyte ghost sample. The d_s and d'_s values obtained from these fits are included in Table 1. The estimated d_s values provided sharper contrast between different samples, which may be in part due to the factors described above.

Using Eq. (7), one dimensional projections of the average probabilities were computed. The reconstructed propagators are shown on the left column of Fig. 5. Note that the speculated scaling behavior of the average propagators in Eq. (12) implies that when the $\overline{P}(z,\Delta)\Delta^{d'_s/2}/z^{d'_f-1}$ values (for positive z) are plotted as a function of $z/\Delta^{1/d_w}$ all average propagators should collapse onto the same curve. This 'collapse' of the probability density values is clearly observed as shown on the right column of Fig. 5. However, a slight divergence in the curves corresponding to long diffusion times was observed towards the right of the figures.

[4] Note that as $\delta/\Delta \to 0$, this relationship reduces to $E(q,\Delta) = \exp(-2\pi^2 q^2\langle z^2\rangle)$, which is consistent with Eq. (10).

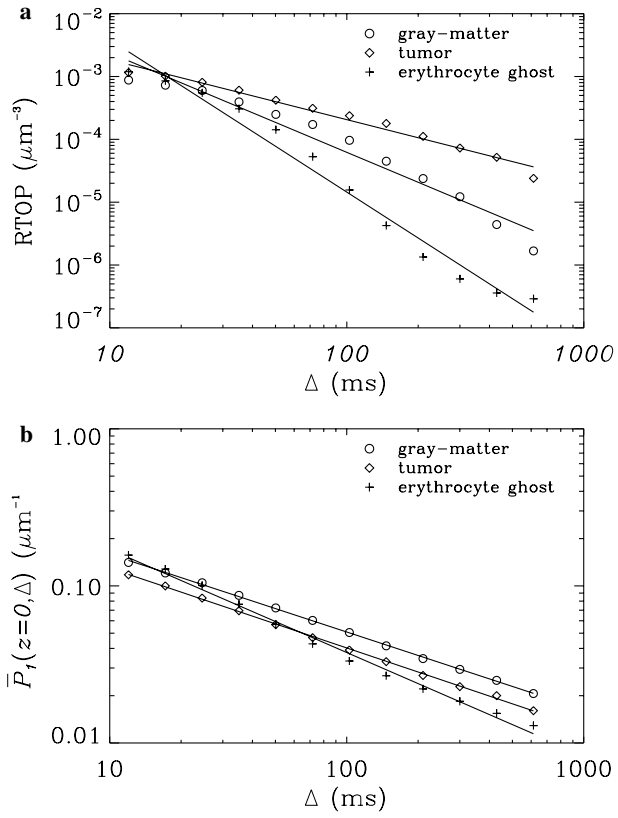

Fig. 4. Diffusion time dependence of the return-to-origin probabilities (a) and the probability of the particles to end up on the xy-plane (b). The slopes of the fitted lines are related to d_s and d'_s, respectively.

Note that only every other time point was included in these plots for the sake of clarity.

5. Discussion

In this work, we demonstrated that a simple model describing anomalous diffusion in disordered media can be employed with success to characterize the diffusion-time dependence of the MR signal attenuation curves obtained from excised biological tissue. Because it is determined by the signal at low q-values, the scaling exponent d_w is sensitive to the large displacement and short time regimes of diffusion. In the context of fractals, it represents the fractal dimension for the trajectories followed by randomly moving particles. On the contrary, the exponent d_s is influenced by the long time return-to-origin-probabilities. When random motion is assumed to be taking place in a fractal space, it quantifies the scaling behavior of the number of visited sites by the random walker [37]. These estimated scaling exponents have great potential as new features that may be sensitive to microscopic alterations of the tissue resulting from development, aging and various pathologies. Our experiments on three different tissue samples demonstrated such a difference. Note, however, that the extent of the study was limited making it difficult to make meaningful inferences about how the tissue state was reflected on the scaling exponents and this was not the intended goal of the study. Rather, the important point in this pilot study is that the proposed methodology did characterize the time evolution of the average propagators well as reflected in the quality of the fits, the consistency of several estimation methods, and the collapse of the average propagators onto single master curves. These findings demonstrate the adequacy and the potential utility of the approach.

Note that potential obstacles to the success of the present study included the finite diffusion gradient pulse duration, δ, i.e. violating the narrow pulse approximation, and associating the diffusion time with the diffusion pulse separation Δ. These issues did not appear to create a significant deviation from the expected scaling behavior, which is valid in the $\delta \ll \Delta$ regime. Another issue that one should be aware of is the assumption about the isotropy of the propagator. Although, from a practical point of view, the method can be applied to one-dimensional q-space data from anisotropic structures as well, the employed model is valid essentially for isotropic structures. It is likely that in anisotropic samples, the estimates of the scaling exponents will depend on the gradient direction. Particularly, one would expect the spectral dimension to have a more significant dependence on the gradient orientation since it is affected by the signal values at high q-values.

Compared to the studies performed to estimate the fractal dimension [38] using the fringe field NMR methods [39], the method introduced here may be more practical. Moreover, it is, in principle, possible to extend the approach to MR imaging of neural tissue and create maps of the d_w and d_s exponents and investigate the spatial variations of these quantities. Note that the estimation of d_w is particularly easy since it requires only two data points near $q = 0$. However, in order to get an accurate estimate of d_s, or describe the temporal evolution of the reconstructed propagators, one has to have a reasonably dense sampling of q-space and cover a large enough distance along the q-axis, which may make the application of the method more difficult to achieve in clinical studies. The approach used here, when restricted to the estimation of d_w, is realizable for a clinical setting since the estimation of d_w requires low q-values and only a few number of scans. However, one should still be cautious since the diffusion pulse duration will probably be longer than presented here, which could introduce some bias in the estimated d_w values.

In fractal spaces, Brownian motion of particles are restricted in all length scales. Similarly in neural tissue, water motion is restricted at different length scales by macromolecules, cytoskeleton, cell membranes, organelles and myelin. It is of great importance to understand to what extent these factors contribute to the anomalous behavior of diffusing particles. Ongoing research is trying to address this point.

6. Conclusion

A simple model that describes diffusion in random disordered media and fractal spaces was used to parameterize

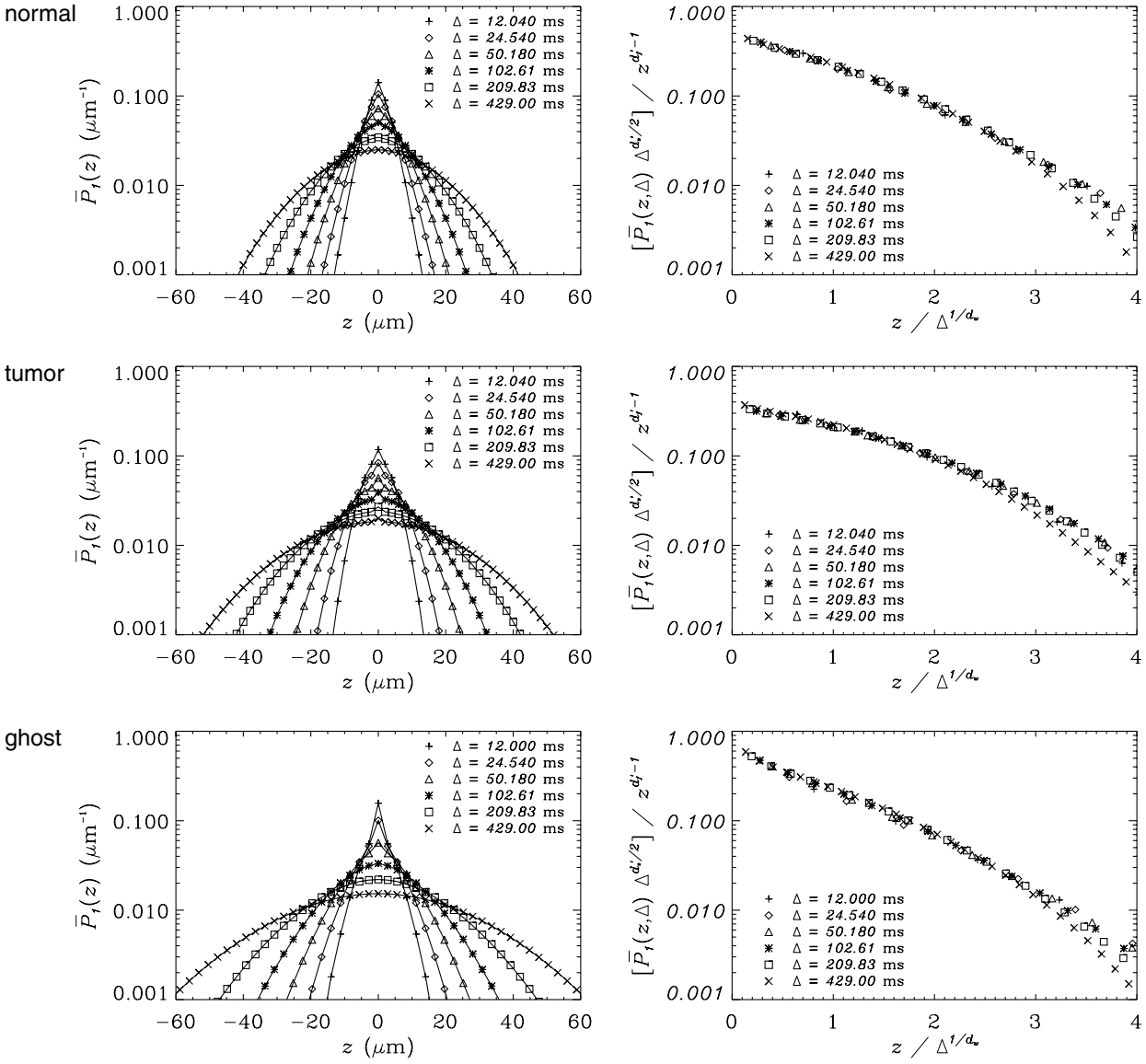

Fig. 5. On the left are the average propagators obtained by transforming the MR signal attenuations for different diffusion times. On the right are the same probability values plotted in a different way based on the form of the propagator as shown in Eq. (12). The propagators for each of the normal gray-matter, glioblastoma and erythrocyte ghost samples are included (from top to bottom). Every other time point of the entire data sets is excluded for clarity.

the diffusion-time dependence of diffusion-weighted MR signals. The model performed well on data obtained from three different biological tissues with different predicted diffusional characteristics. This approach has potential to be applied in clinical studies and may aid in monitoring the developmental as well as pathological changes to biological tissues.

Acknowledgments

We thank Drs. George H. Weiss, Daniel ben-Avraham and Ralph J. Nossal for stimulating discussions. The human tissue was obtained with the help of Drs. Jingxin Qiu, Anthony Yachnis and Thomas Eskin. All MRI data were obtained at the Advanced Magnetic Resonance Imaging and Spectroscopy (AMRIS) facility in the McKnight Brain Institute at the University of Florida. This research was supported by the Intramural Research Program of NICHD, National Institutes of Health Grants R01-NS42075, R01-NS36992 and P41-RR16105, and the National High Magnetic Field Laboratory (NHMFL), Tallahassee.

Appendix A

Since the q-space NMR experiments have limited coverage in q-space, and the estimation of the spectral dimension requires the computation of an integral on the infinite domain, it may be possible to improve the estimation of d_s and d'_s by extrapolating the signal attenuation curves. Among various alternatives, we have achieved satisfactory fits by assuming a signal attenuation of the form

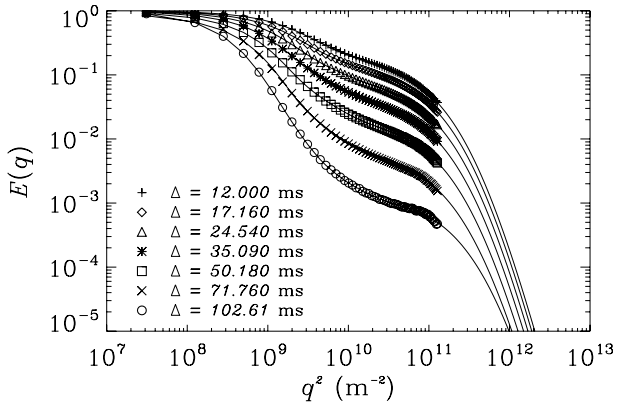

Fig. 6. The signal attenuation values for the erythrocyte ghost sample and the curves obtained by fitting the expression in Eq. (18).

$$E(q,\Delta) = f_1 e^{-uq^2} + f_2 e^{-(vq^2)^{\alpha}} + f_3(1+wq^2)^{-\eta}. \quad (18)$$

In this function the first term is a Debye relaxation expression, whereas the second term is a Kohlrausch–Williams–Watts function [40,41]. Finally the third term is a Rigaut-type asymptotic fractal expression [42]. The fits obtained from the erythrocyte ghost sample are shown in Fig. 6. Note that the fits appear linear in the extrapolated (large-q) region, which indicates that in this regime the function is dominated by the third term in the above expression. This indicates the power-law dependence of the signal attenuation on the gradient strength. This is the expected decay of MR signal in porous media [43].

We have employed this fit in the computation of integrals as described. However, in order not to introduce too much bias due to the particular form of the function, the original data points were not replaced with those as would be required by the above function. Rather, the values of the fitted function were used merely to extend the q-values beyond the acquisition range. Although there may be some bias due to the particular choice for the function, the employed extrapolation may provide an indication about the influence of the finite sampling on the estimated scaling exponents.

References

[1] D. LeBihan, Molecular diffusion, tissue microdynamics and microstructure, NMR Biomed. 8 (7–8) (1995) 375–386.
[2] M.E. Moseley, Y. Cohen, J. Mintorovitch, L. Chileuitt, H. Shimizu, J. Kucharczyk, M.F. Wendland, P.R. Weinstein, Early detection of regional cerebral ischemia in cats: comparison of diffusion and T_2-weighted MRI and spectroscopy, Magn. Reson. Med. 14 (1990) 330–346.
[3] S. Warach, M. Boska, K.M. Welch, Pitfalls and potential of clinical diffusion-weighted MR imaging in acute stroke, Stroke 28 (3) (1997) 481–482.
[4] P.J. Basser, J. Mattiello, D. LeBihan, Estimation of the effective self-diffusion tensor from the NMR spin echo, J. Magn. Reson. B 103 (3) (1994) 247–254.
[5] Y. Assaf, A. Mayk, Y. Cohen, Displacement imaging of spinal cord using q-space diffusion-weighted MRI, Magn. Reson. Med. 44 (5) (2000) 713–722.
[6] J.-H. Lee, C.S. Springer, Effects of equilibrium exchange on diffusion-weighted NMR signals: the diffusigraphic "shutter-speed", Magn. Reson. Med. 49 (3) (2003) 450–458.
[7] P.T. Callaghan, Pulsed field gradient nuclear magnetic resonance as a probe of liquid state molecular organization, Aust. J. Phys. 37 (1984) 359–387.
[8] T. Niendorf, R.M. Dijkhuizen, D.G. Norris, M. van Lookeren Campagne, K. Nicolay, Biexponential diffusion attenuation in various states of brain tissue: implications for diffusion-weighted imaging, Magn. Reson. Med. 36 (6) (1996) 847–857.
[9] G.J. Stanisz, A. Szafer, G.A. Wright, R.M. Henkelman, An analytical model of restricted diffusion in bovine optic nerve, Magn. Reson. Med. 37 (1) (1997) 103–111.
[10] J. Pfeuffer, U. Flögel, W. Dreher, D. Leibfritz, Restricted diffusion and exchange of intracellular water: theoretical modelling and diffusion time dependence of 1H NMR measurements on perfused glial cells, NMR Biomed. 11 (1) (1998) 19–31.
[11] T.G. Smith, W.B. Marks, G.D. Lange, W.H. Sheriff, E.A. Neale, A fractal analysis of cell images, J. Neurosci. Methods 27 (2) (1989) 173–180.
[12] F. Caserta, H.E. Stanley, W. Eldred, G. Daccord, R. Hausman, J. Nittmann, Physical mechanisms underlying neurite outgrowth: a quantitative analysis of neuronal shape, Phys. Rev. Lett. 64 (1) (1990) 95–98.
[13] F. Caserta, W.D. Eldred, E. Fernandez, R.E. Hausman, L.R. Stanford, S.V. Bulderev, S. Schwarzer, H.E. Stanley, Determination of fractal dimension of physiologically characterized neurons in two and three dimensions, J. Neurosci. Methods 56 (2) (1995) 133–144.
[14] S. Havlin, S.V. Buldyrev, A.L. Goldberger, R.N. Mantegna, S.M. Ossadnik, C.K. Peng, M. Simons, H.E. Stanley, Fractals in biology and medicine, Chaos Solitons Fractals 6 (1995) 171–201.
[15] D. ben-Avraham, S. Havlin, Diffusion and Reactions in Fractals and Disordered Systems, Cambridge University Press, Cambridge, UK, 2000.
[16] Y. Gefen, A. Aharony, S. Alexander, Anomalous diffusion on percolating clusters, Phys. Rev. Lett. 50 (1) (1983) 77–80.
[17] A. Klemm, R. Metzler, R. Kimmich, Diffusion on random-site percolation clusters: theory and NMR microscopy experiments with model objects, Phys. Rev. E 65 (2) (2002) 021112.
[18] B. Buhai, A. Hakimov, I. Ardelean, R. Kimmich, NMR acceleration mapping in percolation model objects, J. Magn. Reson. 168 (2004) 175–185.
[19] H.P. Müller, J. Weis, R. Kimmich, Computer simulation and six-dimensional spin density and velocity NMR microimaging of lacunar systems: a comparative analysis of percolation properties, Phys. Rev. E 52 (5) (1995) 5195–5204.
[20] H.P. Müller, R. Kimmich, J. Weis, NMR flow velocity mapping in random percolation model objects: evidence for a power-law dependence of the volume-averaged velocity on the probe-volume radius, Phys. Rev. E 54 (5) (1996) 5278–5285.
[21] T. Zavada, N. Südland, R. Kimmich, T.F. Nonnenmacher, Propagator representation of anomalous diffusion: the orientational structure factor formalism in NMR, Phys. Rev. E 60 (2) (1999) 1292–1298.
[22] D.G. Cory, A.N. Garroway, Measurement of translational displacement probabilities by NMR: an indicator of compartmentation, Magn. Reson. Med. 14 (3) (1990) 435–444.
[23] P.T. Callaghan, Principles of Nuclear Magnetic Resonance Microscopy, Clarendon Press, Oxford, 1991.
[24] Y. Cohen, Y. Assaf, High b-value q-space analyzed diffusion-weighted MRS and MRI in neuronal tissues—a technical review, NMR Biomed. 15 (2002) 516–542.
[25] M.D. Hürlimann, L.M. Schwartz, P.N. Sen, Probability of return to origin at short times: a probe of microstructure in porous media, Phys. Rev. B 51 (21) (1995) 14936–14940.
[26] S. Havlin, D. ben Avraham, Diffusion in disordered media, Adv. Phys. 51 (1) (2002) 187–292.
[27] P.N. Sen, Time-dependent diffusion coefficient as a probe of geometry, Concept Magn. Reson. A 23A (1) (2004) 1–21.

[28] L.L. Latour, K. Svoboda, P.P. Mitra, C.H. Sotak, Time-dependent diffusion of water in a biological model system, Proc. Natl. Acad. Sci. USA 91 (1994) 1229–1233.
[29] P.E. Thelwall, S.C. Grant, G.J. Stanisz, S.J. Blackband, Human erythrocyte ghosts: exploring the origins of multiexponential water diffusion in a model biological tissue with magnetic resonance, Magn. Reson. Med. 48 (4) (2002) 649–657.
[30] W.H. Press, S.A. Teukolsky, W.T. Vetterling, B.P. Flannery, Numerical Recipes in C: The Art of Scientific Computing, Cambridge Press, Cambridge, 1992.
[31] J.R. Banavar, M. Lipsicas, J.F. Willemsen, Determination of the random-walk dimension of fractals by means of NMR, Phys. Rev. B 32 (9) (1985) 6066.
[32] G. Jug, Theory of NMR field-gradient spectroscopy for anomalous diffusion in fractal networks, Chem. Phys. Lett. 131 (1,2) (1986) 94–97.
[33] J. Kärger, G. Vojta, On the use of NMR pulsed field-gradient spectroscopy for the study of anomalous diffusion in fractal networks, Chem. Phys. Lett. 141 (5) (1987) 411–413.
[34] J. Kärger, H. Pfeifer, G. Vojta, Time correlation during anomalous diffusion in fractal systems and signal attenuation in NMR field-gradient spectroscopy, Phys. Rev. A 37 (11) (1988) 4514–4517.
[35] A. Widom, H.J. Chen, Fractal Brownian motion and nuclear spin echoes, J. Phys. A 28 (1995) 1243–1247.
[36] B.H. Kaye, Multifractal description of a rugged fineparticle profile, Part Charact. 1 (1984) 14–21.
[37] H.E. Stanley, Fractals and multifractals: the interplay of physics and geometry, in: A. Bunde, S. Havlin (Eds.), Fractals and Disordered Systems, Springer-Verlag, Berlin, 1991, pp. 1–49, Ch. 1.
[38] M. Köpf, C. Corinth, O. Haferkamp, T.F. Nonnenmacher, Anomalous diffusion of water in biological tissues, Biophys. J. 70 (1996) 2950–2958.
[39] R. Kimmich, W. Unrath, G. Schnur, E. Rommel, NMR measurement of small self-diffusion coefficients in the fringe field of superconducting magnets, J. Magn. Reson. 91 (1) (1991) 136–140.
[40] R. Kohlrausch, Über das Dellmann'sche Elektrometer, Ann. Phys. 72 (1847) 393–405.
[41] K.M. Bennett, K.M. Schmainda, R. Bennett(Tong), D.B. Rowe, H. Lu, J.S. Hyde, Characterization of continuously distributed cortical water diffusion rates with a stretched-exponential model, Magn. Reson. Med. 50 (4) (2003) 727–734.
[42] M. Köpf, R. Metzler, O. Haferkamp, T.F. Nonnenmacher, NMR studies of anomalous diffusion in biological tissues: experimental observation of Lévy stable processes, in: G.A. Losa, D. Merlini, T.F. Nonnenmacher, E.R. Weibel (Eds.), Fractals in Biology and Medicine, vol. 2, Birkhäuser, Basel, 1998.
[43] P.N. Sen, M.D. Hürlimann, T.M. de Swiet, Debye-Porod law of diffraction for diffusion in porous media, Phys. Rev. B 51 (1) (1995) 601–604.